



Design of ketone derivatives as highly efficient photoinitiators for free radical and cationic photopolymerizations and application in 3D printing of composites

Yangyang Xu, Zhaofu Ding, Haibin Zhu, Bernadette Graff, Stephan Knopf, Pu Xiao, Frédéric Dumur, Jacques Lalevée

► To cite this version:

Yangyang Xu, Zhaofu Ding, Haibin Zhu, Bernadette Graff, Stephan Knopf, et al.. Design of ketone derivatives as highly efficient photoinitiators for free radical and cationic photopolymerizations and application in 3D printing of composites. *Journal of Polymer Science*, John Wiley & Sons, 2020, 58 (24), pp.3432-3445. 10.1002/pol.20200658 . hal-03078875

HAL Id: hal-03078875

<https://hal.archives-ouvertes.fr/hal-03078875>

Submitted on 16 Dec 2020

HAL is a multi-disciplinary open access archive for the deposit and dissemination of scientific research documents, whether they are published or not. The documents may come from teaching and research institutions in France or abroad, or from public or private research centers.

L'archive ouverte pluridisciplinaire **HAL**, est destinée au dépôt et à la diffusion de documents scientifiques de niveau recherche, publiés ou non, émanant des établissements d'enseignement et de recherche français ou étrangers, des laboratoires publics ou privés.

Design of ketone derivatives as highly efficient photoinitiators for free radical and cationic photopolymerizations and application in 3D printing of composites

Yangyang Xu,^{a,b,c*} Zhaofu Ding,^a Haibin Zhu,^a Bernadette Graff,^{b,c} Stephan Knopf^{2,3} Pu Xiao,^{d*} Frédéric Dumur^{e*} and Jacques Lalevée^{b,c*}

^aCollege of Chemistry and Materials Science, Anhui Normal University, South Jiu Hua Road 189, Wuhu 241002, China. E-mail: ahnuxy@ahnu.edu.cn

^bUniversité de Haute-Alsace, CNRS, IS2M UMR 7361, F-68100 Mulhouse, France. E-mail: jacques.lalevee@uha.fr

^cUniversité de Strasbourg, France.

^dResearch School of Chemistry, Australian National University, Canberra, ACT 2601, Australia. E-mail: pu.xiao@anu.edu.au

^eAix Marseille Univ, CNRS, ICR UMR 7273, F-13397 Marseille, France. E-mail: Frederic.dumur@univ-amu.fr

Abstract: Chalcones correspond to a scaffold present in many natural products and are well-known to exhibit a strong absorption in the near-UV/visible region. Herein, thirteen ketone derivatives (ketone-1~ketone-13) based on this latter scaffold were designed, remarkably, 10 of the ketones were never synthesized before. These ketones are proposed as high-performance photoinitiators for both free radical polymerizations and cationic polymerizations under soft conditions (visible LED@405 nm irradiation at room temperature). In combination with an amine and an iodonium salt (Iod), these ketones could be used in three-component photoinitiating systems to initiate the free radical polymerization of acrylates with distinct final conversions, among which the ketone-1/amine/Iod combination proved to be the most efficient one. Besides, the ketone-1/Iod two-component system also showed a remarkable photoinitiation ability for the cationic polymerization of epoxides. The photochemical sensitivity of ketone-1 in the presence of an amine and an iodonium salt was systematically investigated by steady state photolysis and excited state fluorescence quenching characterizations, respectively. Interestingly, macroscopic 3D patterns with excellent spatial resolution could be generated using the ketone-1/amine/Iod photoinitiating system for the free radical polymerization of acrylates. This high performance is found useful to overcome the light penetration issue for the access to filled samples (silica) and the preparation of composites.

1. Introduction

Photopolymerization reactions induced by light possess some intrinsic advantages when compared with conventional thermal-induced reactions, including fast polymerization rates, room temperature operation, low energy consumption, remote controllability and environmental friendly operating conditions without volatile organic compounds emission.^{1–5} Photopolymerization can also be considered as offering a green access to polymers when the appropriate light sources are used. Especially, the development of photocurable formulations sensitive to visible light-emitting diodes (LEDs) has attracted a great deal of attention from researchers.^{6–8} The LED technology has rapidly evolved and gained much popularity in recent years thanks to its inherent merits: high-quality illumination and efficiency, adjustable intensity, no ozone release, long lifespan and endurance, safe usage conditions and minimal heat generation as well as fewer harmful UV rays.^{9–11} Although achievements for certain photosensitive formulations using LEDs can be found in the literature, the exploration for high-performance photoinitiators or photoinitiating systems upon exposure to near-UV/visible LEDs still remains a huge challenge.^{12,13}

3D printing technology, also known as an additive manufacturing technology, has witnessed intense research efforts and its scope of application has rapidly evolved from the traditional manufacturing fields to biomedical engineering, radiology, electronics, photonics, precision machinery and other high-tech fields.^{14–17} In order to ensure a safe and economical irradiation set-up for 3D printing based on stereolithography, the 405 nm wavelength is now widely recognized as the reference wavelength.^{18,19} However, one huge obstacle for photocuring 3D printing is that the existing photoinitiators are not fully adapted to the current irradiation wavelength of 405 nm.²⁰ Therefore, the development of efficient photosensitive 3D printing systems activable at 405 nm wavelength is extremely desired. The ketone moiety based on the chalcone scaffold is well known for the light absorption in the near-UV/visible region, and found as a promising structure for the design of effective photoinitiators to initiate photopolymerization reactions.^{21,22} In this context, it's of great significance to develop ketone derivatives with a strong absorbance in the near UV/visible region (*e.g.* 405 nm) through rational molecular structure design (*i.e.* molecular modeling). Thus, these ketones would find a widespread application prospect in photopolymerization reactions under mild conditions as well as 3D printing with 405 nm LEDs. For filled samples, the light diffusion (or absorption) by the fillers strongly limits the light penetration. Therefore, the development of highly efficient systems able to polymerize in depth (*e.g.* with low light intensity) is highly desired in the preparation of composites.

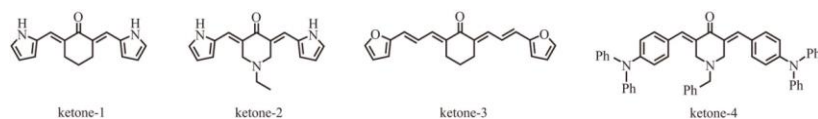
In the present work, a new series of ketone derivatives (noted as ketone-1~ketone-13) have been *in silico* designed through molecular modeling calculations and investigated as visible light sensitive photoinitiators. Remarkably, 10 of the ketones were never synthesized before and only ketones 1, 3 and 4 were already prepared but for other fields (*i.e.* never studied as photoinitiators). The different peripheral substituents and central cyclohexanones determined not only the absorption properties but also the photochemical properties of the targeted ketones. In the presence of photo-additives or co-initiators, the newly proposed ketones were incorporated into two- and

three-component photoinitiating systems for cationic polymerization and free radical polymerization, respectively. Remarkable photoinitiation properties in terms of photopolymerization profiles, final reactive function conversions and photopolymerization rates have been noted for these ketone derivatives. Particularly, the high photoinitiation ability of ketone-1 was further reflected in the photocuring 3D printing experiments with acrylates. As example of this high reactivity, the access to composites is also presented.

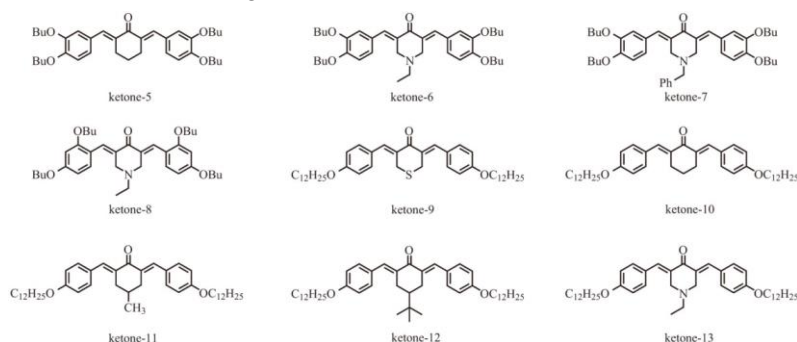
2. Experimental section

2.1. Materials

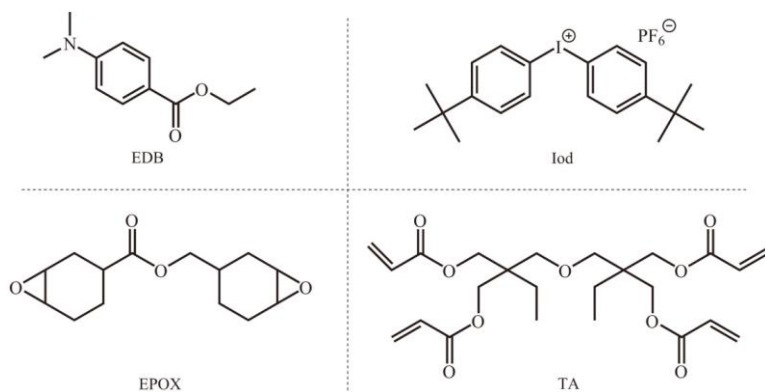
Ketone derivatives containing different cyclohexanone central cores and peripheral substituting groups were synthesized according to the procedures described in detail in the ESI and their corresponding chemical structures are depicted in Scheme 1 (ketone-1~ketone-4) and Scheme 2 (ketone-5~ketone-13). Both the amine (ethyl 4-(dimethylamino)benzoate-EDB) and the iodonium salt (di-*tert*-butyldiphenyl iodonium hexafluorophosphate-Iod, commercial name: Speedcure 938) were obtained from Lambson Ltd. Di(trimethylolpropane) tetraacrylates (TA) and 3,4-Epoxy cyclohexylmethyl 3,4-epoxycyclohexanecarboxylate (EPOX, commercial name: Uvacure® 1500) were purchased from Allnex and used as the benchmark monomers for the free radical polymerization and cationic polymerization, respectively. The molecular structures of all these commercially available chemicals are shown in Scheme 3, and they were selected with the highest purity and used as received.



Scheme 1. Chemical structures of the four ketone derivatives with maximum absorbance at the visible region.



Scheme 2. Chemical structures of the other nine ketone derivatives with maximum absorbance at the UV region.



Scheme 3. Chemical structures of the photo-additives (EDB and iodonium salt/Iod) as well as EPOX and TA acting as benchmark monomers.

2.2. Formulation preparation

The weight percent of the ketones-based photoinitiating systems are given in comparison to the monomer content and the basic formulation is presented in Table S1. For the free radical polymerization, different ketones, amine and iodonium salt (0.1%/2%/2%, w/w/w) were successively added into colorless TA resin. Then, upon the strong mechanical mixing by a SpeedMixer (DAC 150.1 FVZ-K) with rotation speed at 2000 rpm for several minutes, a homogeneous resin could be produced (Fig. S1). For the cationic polymerization, different ketones and the iodonium salt (0.1%/2%, w/w) were mixed together into EPOX, and a homogeneous resin could be produced after the mechanical mixing with the same SpeedMixer for several minutes. Notably, the final formulations exhibited different colors due to the presence of different ketone derivatives.

2.3. Irradiation source

Both the free radical polymerization and the cationic polymerization were conducted under a visible LED irradiation with the maximum emission wavelength at 405 nm ($\lambda_{\text{emi}}=405$ nm). The same LED@405 nm was also utilized as the irradiation source for the photolysis experiments. And the incident light intensity of the visible LED at the surface of sample was set about 110 mW/cm².

2.4. Real-time Fourier transform infrared (RT-FTIR) spectroscopy

All the photopolymerization experiments were carried out under mild conditions: visible LED@405 nm irradiation at room temperature. One drop of the prepared formulation was deposited between two polypropylene films (in laminate) to reduce the oxygen inhibition effect with about 25 μm in thickness (the thickness is controlled from the FTIR spectra). And the real time Fourier transform infrared spectroscopy (RT-FTIR, JASCO FTIR 4100) was utilized to quantitatively characterize the photopolymerization kinetics by continuously following the evolution of the reactive groups: double bond content of TA (C=C at 1630 cm⁻¹) and the epoxide group content of EPOX (monitored

at $\sim 795\text{ cm}^{-1}$), respectively.²³ The final conversion (FC) of the reactive functional groups was determined by comparing the peak area of the relevant characteristic IR peaks for a certain LED irradiation time:

$$\text{FC (\%)} = [A_0 - A_t] / A_0 \times 100 \quad (1)$$

where A_0 is the initial peak area of reactive groups before LED@405 nm irradiation, while A_t is the corresponding peak area after the LED irradiation for a certain time t .

2.5. UV-visible absorption spectroscopy and steady state photolysis characterization

UV-visible absorption properties of the thirteen designed ketones as well as the steady state photolysis experiments were investigated in a quartz cuvette with an optical path of 1.0 cm by a JASCO V730 UV-visible spectrometer. Acetonitrile served as a good solvent for the characterization, and the specific experimental conditions are given in the corresponding figures. Absorbance data were converted into molar extinction coefficients (ϵ) and expressed in classical units [$\text{M}^{-1}\text{ cm}^{-1}$].

2.6. Fluorescence quenching experiments

Fluorescence properties of the different ketones and the fluorescence quenching experiments were studied in acetonitrile with JASCO FP-6200 spectrofluorimeter. The excitation wavelength was set at 410 nm, and the specific experimental conditions are given in the corresponding figures.

2.7. Computational procedure

UV-visible spectra and the frontier orbitals (Highest Occupied Molecular Orbital-HOMO and Lowest Unoccupied Molecular Orbital-LUMO) were calculated at Density Functional Theory (DFT) level using the Gaussian 09 software. The procedure was presented in our previous paper.²⁴

2.8. Laser write experiments

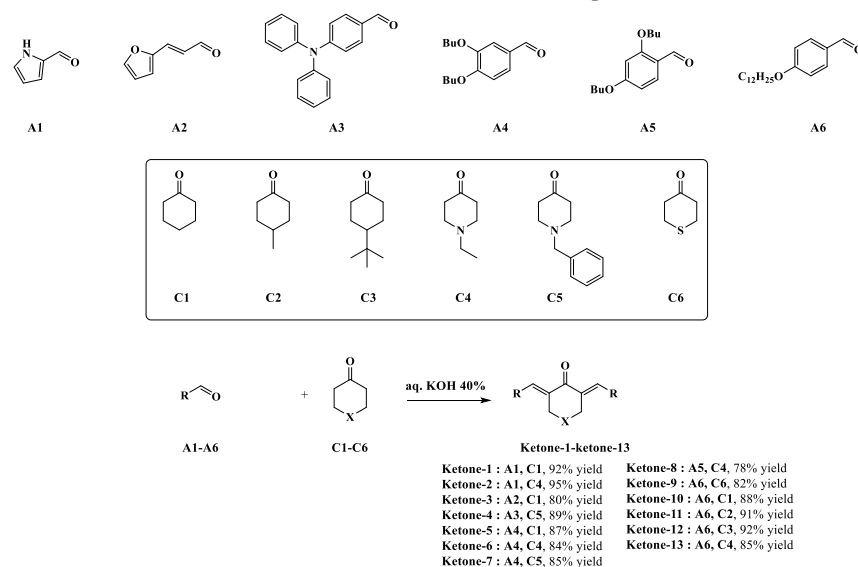
The TA resin containing ketone-based three-component photoinitiating system was deposited into a homemade tank. A computer programed laser diode (Thorlabs) with maximum emission wavelength also at 405 nm was selected as the irradiation source for the spatially controlled photocuring process. The spot size of the laser was about 50 μm and the intensity of the laser at sample's surface was about 110 mW. The laser write experiments of the resin were conducted under air at room temperature to generate 3D patterns. Fabricated 3D patterns were observed and analyzed via a numerical optical microscope (DSX-HRSU, OLYMPUS corporation).

3. Results and discussion

3.1 Synthesis of the thirteen ketone derivatives

The thirteen ketone derivatives, denoted as ketone-1~ketone-13, are composed of different central cyclohexanones and peripheral substituting groups. The general synthetic routes towards these ketones are depicted in Scheme 4, meanwhile the detailed synthetic procedures and structural analysis of the targeted ketones are

described in the ESI. Briefly, all chalcones were prepared by a Claisen–Schmidt condensation reaction under strongly basic conditions (aq. 40% KOH). Ketone-1~ketone-13 could be obtained with reaction yields ranging from 78% for ketone-8 to 95% for ketone-2. Except ketones-1, 3 and 4 that were previously reported in the literature, the other ten structures have never been reported before.



Scheme 4. General synthetic routes towards the thirteen ketone derivatives.

3.2. UV–visible absorption property of the designed ketone derivatives

The ground-state absorption spectra of the thirteen proposed ketone derivatives were examined in acetonitrile and the different spectra are shown in Fig. 1. It seems that the different structures of the peripheral substituting chromophores and central cyclohexanone cores bring a huge impact on the absorption properties of the newly designed ketone derivatives. As can be seen in Fig. 1, all ketones displayed a strong absorption in the near-UV/visible region and the dyes are characterized by various values of maximum absorbance and molar extinction coefficients in a broad wavelength range. The thirteen ketone derivatives can be mainly categorized into two groups: (1) the ketone-1~ketone-4 showed a maximum absorption in the visible region, located between 405 nm and 435 nm; Conversely, (2) the ketone-5~ketone-13 exhibited a maximum absorption in the near-UV region between 350 nm and 375 nm. Absorption maxima (λ_{max}) as well as the molar extinction coefficients at λ_{max} (ϵ_{max}) and at 405 nm ($\epsilon_{405 \text{ nm}}$) are summarized in the Table 1. The light absorption properties of all ketones demonstrate certain degrees of overlap with the maximum emission wavelength (*i.e.* 405 nm) of the visible LED used in this work. Remarkably, both ketone-2 and ketone-3 showed the highest molar extinction coefficients at 405 nm, which are over $36,000 \text{ M}^{-1} \text{ cm}^{-1}$. Besides, ketone-1 and ketone-4 also showed a relatively strong absorbance at 405 nm with $\epsilon_{405 \text{ nm}}$ values over $17,000 \text{ M}^{-1} \text{ cm}^{-1}$. These ketones show clear π - π^*

transitions (see the frontier orbitals in Figure 2) with a partial charge transfer character for ketone 4 (see HOMO-LUMO - Figure 2) in agreement with a higher bathochromic shift for this latter structure. However, for ketone-5~ketone-13, lower $\epsilon_{405\text{ nm}}$ values are observed, which are in a wide range from 900 $\text{M}^{-1}\text{ cm}^{-1}$ to 16,000 $\text{M}^{-1}\text{ cm}^{-1}$. It's believed that the different absorption properties of these ketones would play a very important role in their photoinitiation abilities for the free radical and cationic photopolymerizations.²⁵

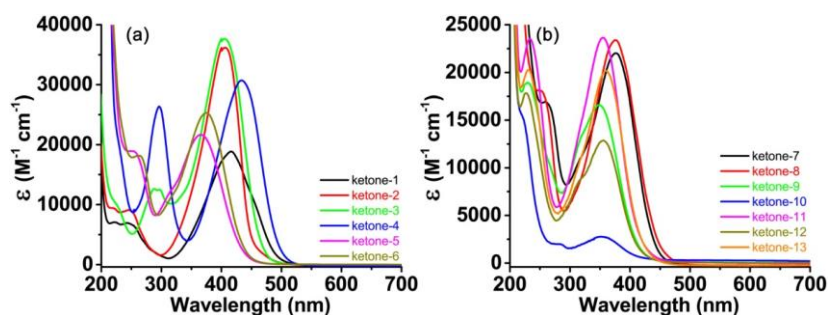


Figure 1. UV-visible absorption property of the thirteen ketone derivatives dissolved in acetonitrile: (a) for ketone-1~ketone-6 and (b) for ketone-7~ketone-13, respectively.

Table 1. Summary of the light absorption properties of the investigated ketone derivatives: maximum absorption wavelengths (λ_{max}) and molar extinction coefficients at λ_{max} (ϵ_{max}) and 405 nm ($\epsilon_{405\text{ nm}}$), respectively.

	λ_{max} (nm)	ϵ_{max} ($\text{M}^{-1}\text{ cm}^{-1}$)	$\epsilon_{405\text{ nm}}$ ($\text{M}^{-1}\text{ cm}^{-1}$)
ketone-1	416	18800	17900
ketone-2	405	36200	36200
ketone-3	405	37700	37700
ketone-4	434	30800	23000
ketone-5	366	21700	11100
ketone-6	375	25200	15500
ketone-7	375	22000	14500
ketone-8	375	23400	15800
ketone-9	350	16500	3100
ketone-10	350	2800	900
ketone-11	355	23600	5300
ketone-12	355	12900	2700
ketone-13	360	20200	5700

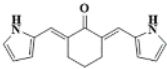


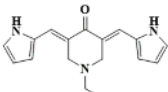
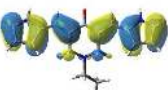

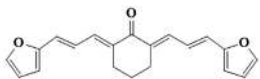


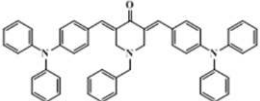


	HOMO	LUMO
(ketone-1) 		
(ketone-2) 		
(ketone-3) 		
(ketone-4) 		

Figure 2. Frontier molecular orbitals (HOMOs and LUMOs) for ketone-1 to ketone-4; structures optimized at the B3LYP/6-31G* level of theory.

3.3. Free radical photopolymerization of TA

Previous researches have reported that neither amine nor iodonium salt alone could be able to initiate the free radical polymerization of acrylates, due to the lack of absorbance beyond 300 nm.^{26,27} Firstly, the ketone derivatives (0.1%, w) were tried alone as single photoinitiators to initiate the free radical polymerization of TA, a tetrafunctional polyether acrylate, but the final conversion (FC) of acrylates was lower than 20% using LED@405 nm as the light source. Then ketone/amine (0.1%/2%, w/w) and ketone/Iod (0.1%/2%, w/w) two-component systems, respectively, were tried for the free radical polymerization under the same polymerization conditions; however, the FCs of acrylates were still not very high (about 40% for the ketone-1/amine system and 55% for the ketone-1/Iod system), as shown in Fig. S2. These blank experiments highlighted the necessity to mix these different chemical compounds for the access to efficient photoinitiating systems. Therefore, the ketone/amine/Iod (0.1%/2%/2%, w/w/w) three-component systems were proposed and investigated for the free radical polymerization of TA under mild conditions: visible LED@405 nm irradiation at room

temperature. And typical acrylate group conversions versus LED irradiation time profiles are depicted in Fig. 3 through the RT-FTIR method performed in laminate. The oxygen inhibition effect could be neglected in this work, since the free radical photopolymerization took place immediately upon the visible LED irradiation. It's clear that, in the control experiment the amine/Iod (2%/2%, w/w) two-component system could only induce a partial polymerization of TA with the FC of acrylates just about 39%. Interestingly, along with the addition of ketones to form three-component systems, the photoinitiation efficiency was greatly enhanced, thus highlighting the essential role of the ketone derivatives for the free radical polymerization. Both the FC values of acrylates and the photopolymerization rates have been improved by a large degree in the presence of the ketone/amine/Iod three-component systems. The FC values of acrylates are summarized in Table 2, and among all the ketones-based three-component photoinitiating systems, the ketone-1/amine/Iod could induce the highest FC value of acrylates, which is about 85%. The IR absorption spectra of TA in the presence of ketone-1/amine/Iod system were recorded and compared during the photopolymerization process (Fig. S3). Before the LED@ 405 nm irradiation, a strong C=C band was observed between 1600 cm^{-1} and 1650 cm^{-1} . While after LED irradiation for 400 s, an obvious intensity decrement happened to this band, further demonstrating the high photoinitiation ability of the ketone-1/amine/Iod three-component photoinitiating system for the free radical polymerization of acrylates. On the contrary, the ketone-4/amine/Iod and the ketone-8/amine/Iod three-component systems could induce the lowest FC value of acrylates, which is just about 56%. The above results indicate that the distinct photoinitiation behaviors of ketones-based three-component systems are not directly linked to their respective absorption properties ($\epsilon_{405\text{ nm}}$). And the photochemical reactivity of these ketones may also play a very important role in their initiating abilities, which will be discussed thoroughly in the following part.²⁸

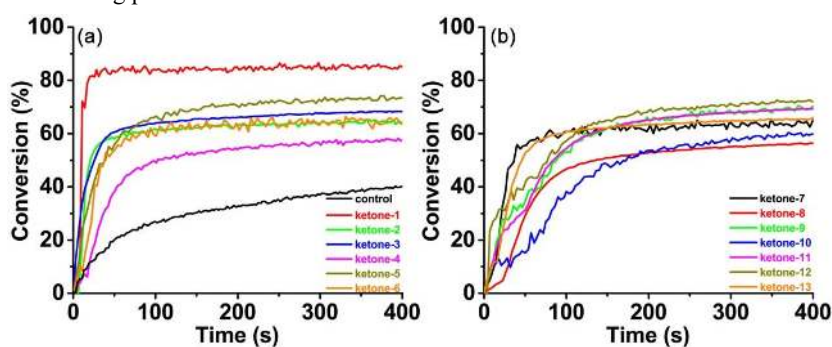


Figure 3. Photopolymerization profiles of TA (C=C conversion vs. irradiation time) upon LED@405 nm irradiation in thin films condition (25 μm) in the presence of different ketone/amine/Iod (0.1%/2%/2%, w/w/w) photoinitiating systems, respectively. For the control experiment, only amine/Iod (2%/2%, w/w) two-component system was tested.

Table 2. Final acrylate function conversions (FCs) in TA upon LED@405 nm irradiation for 400 s in the presence of ketone/amine/Iod (0.1%/2%/2%, w/w/w) three-component photoinitiating systems in thin films condition (25 μm).

	FCs
amine/Iod without ketones	39%
ketone-1	85%
ketone-2	64%
ketone-3	68%
ketone-4	56%
ketone-5	73%
ketone-6	64%
ketone-7	63%
ketone-8	56%
ketone-9	69%
ketone-10	60%
ketone-11	69%
ketone-12	72%
ketone-13	66%

3.4. Cationic photopolymerization of EPOX

Besides the free radical polymerization, the cationic polymerization of epoxides also occupies a large share in polymer materials industry. It would be very promising to check the photoinitiation ability of these ketone derivatives for the cationic polymerization of epoxides. Neither the ketones nor the iodonium salt alone could effectively initiate the cationic polymerization of EPOX using a LED@405 nm as the light source.²⁹ Therefore, the ketone/Iod (0.1%/2%, w/w) two-component systems were proposed for the cationic polymerization, and typical epoxide group conversions versus LED irradiation time profiles are depicted in Fig. 4 through the same RT-FTIR method also performed in laminate. Interestingly, the ketone-1/Iod system could illustrate quite good photoinitiation ability for the cationic polymerization of EPOX with both high FC value (nearly 70%) of epoxides and high polymerization rate. However, in the presence of the iodonium salt under the same irradiation conditions, the other ketones could only result in rather low photoinitiation efficiency for the cationic polymerization of thin EPOX films, and the FC values of epoxides are < 30%. The high photoinitiation ability of ketone-1 for the cationic polymerization of epoxides was further confirmed by recording the IR absorption spectra of EPOX. Before LED@405 nm irradiation, a strong band was detected at 795 cm^{-1} , corresponding to the epoxide group. While after LED irradiation for 400 s, the intensity of epoxide group decreased obviously in the presence of the ketone-1/Iod two-component system. In the meantime, a new peak appeared at about 1084 cm^{-1} , which is ascribed to the formation of a polyether network.^{30,31} The IR spectral changes of EPOX during LED irradiation provide a convincing evidence for the high photoinitiation ability of ketone-1/Iod for the cationic polymerization. All the above results suggest that in combination with additives (iodonium salt, amine) the proposed ketone derivatives could be excellent

photoinitiators for both the free radical polymerization of acrylates and the cationic polymerization of epoxides under mild conditions.

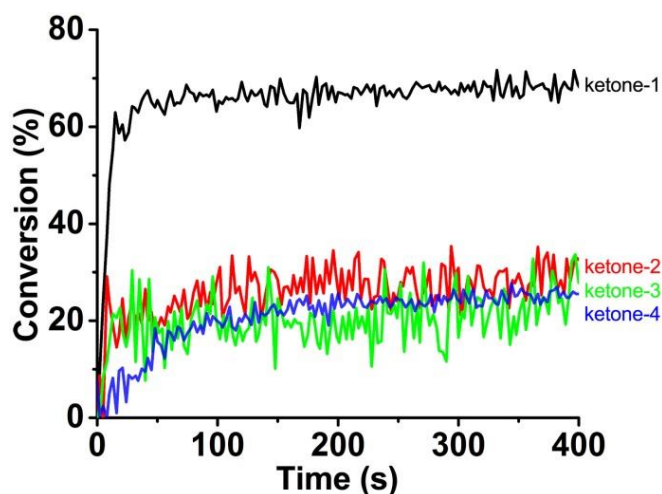


Figure 4. Photopolymerization profiles of EPOX (epoxide function conversion vs. irradiation time) upon LED@405 nm irradiation in thin films condition (25 μm) in the presence of different ketone/Iod (0.1%/2%, w/w) two-component photoinitiating systems at room temperature, respectively.

3.5. Steady state photolysis of ketones

The steady state photolysis characterization provides a powerful method to study the photochemical mechanism of the ketone derivatives involved in the photopolymerization reactions. Ketone-1 showed the strongest photoinitiation ability for both the free radical polymerization and the cationic polymerization, while a weaker photoinitiation ability was observed for ketone-2, although they shared the same peripheral substituting moiety, *i.e.* the pyrrole group. It seems that the different central cyclohexanone cores should take the responsibility for the distinct photoinitiation abilities of these two ketones. No obvious photolysis could be observed if the ketones were kept alone in the absence of any additives. Therefore, ketone-1 and ketone-2 were selected as representative ketone derivatives for the steady state photolysis study in the presence of an amine and an iodonium salt, respectively, through a UV-visible spectrometer. The 405 nm LED was utilized as the irradiation source for the photolysis experiments since the maximum absorbance of ketone-1 and ketone-2 was located in the visible region. The UV-visible absorption spectra of ketone-1 and ketone-2 in combination with an amine (EDB) upon LED@405 nm irradiation are presented in Fig. 5. Before the LED irradiation, these two ketone derivatives showed a strong absorbance between 350 nm–500 nm in the presence of the amine. However, along with the increasing time of LED@405 nm irradiation from 0 to 10 min, a clear intensity decline was observed. Besides, an obvious bathochromic shift also happened for the ketone-1/amine and ketone-2/amine systems (Fig. 5a, 5c). Moreover, based on the

spectral decrement of the maximum absorbance in the UV-visible absorption spectra, the percentage consumption of ketones against LED irradiation time was calculated and presented (see Fig. 5b, 5d). And these two ketones illustrated similar percentage consumptions in the presence of an amine upon LED irradiation for 10 min: about 11% for ketone-1 and 12% for ketone-2.

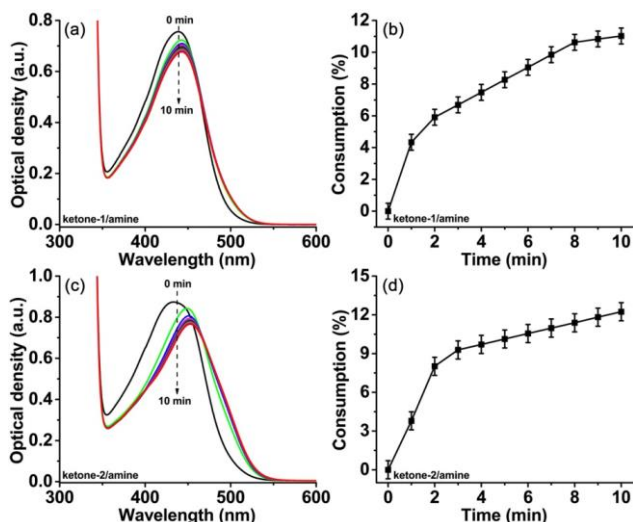


Figure 5. UV-visible absorption spectra of (a) ketone-1 (3.96×10^{-5} M) and (c) ketone-2 (3.55×10^{-5} M) in the presence of amine (EDB, 1.0×10^{-2} M) upon LED@405 nm irradiation in the solvent of acetonitrile; Consumption of ketones for (b) ketone-1/amine and (d) ketone-2/amine two-component systems, respectively.

The steady state photolysis study of ketone-1 and ketone-2 in the presence of the iodonium salt (Speedcure 938) was also performed using the same LED@405 nm as the irradiation source. The UV-visible absorption spectra of ketone-1 and ketone-2 in combination with the iodonium salt upon LED@405 nm irradiation are presented in Fig. 6. Before the LED irradiation, the maximum absorbance of ketone-1 and ketone-2 appeared at 428 nm and 432 nm, respectively. Then, upon the visible LED irradiation from 0 to 10 min, a dramatic intensity decline was observed for the ketone-1/Iod and ketone-2/Iod systems. Besides, an obvious bathochromic shift in the UV-visible absorption spectra was also observed for these two ketone derivatives (Fig. 6a, 6c). Especially, along with the photolysis of ketone-1 in the presence of the iodonium salt, the acetonitrile solution changed from yellow to nearly colorless, as shown in Fig. S4. The percentage consumption of ketones was presented against LED@405 nm irradiation time and a nonlinear growth for the percentage consumption of ketones was detected (see Fig. 6b, 6d). In combination with the iodonium salt, the final consumption of ketone-1 was about 78%, while the final consumption of ketone-2 was just 32%. The above steady state photolysis characterization suggested a strong interaction among the ketone/amine/Iod three-component systems, and an oxidation-reduction

photochemical mechanism was already proposed by our group for other photoinitiators.^{20,25} Moreover, the dramatic difference in the final consumptions of ketones, in the presence of the iodonium salt, indicated that ketone-1 illustrated a much higher photochemical reactivity than ketone-2 under the same irradiation conditions, which could be useful to explain their different photoinitiation abilities for both the free radical polymerization and cationic polymerization.

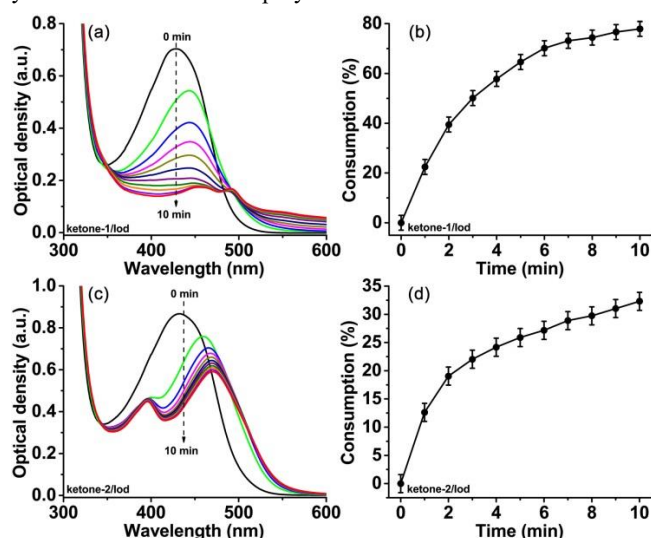


Figure 6. UV–visible absorption spectra of (a) ketone-1 (3.96×10^{-5} M) and (c) ketone-2 (3.55×10^{-5} M) in the presence of the iodonium salt (Speedcure 938, 1.0×10^{-2} M) upon LED@405 nm irradiation in the solvent of acetonitrile; Consumption of ketones for (b) ketone-1/Iod and (d) ketone-2/Iod two-component systems, respectively.

3.6. Excited state fluorescence quenching of ketones

The strong interaction between the ketones and the additives was further verified by the fluorescence quenching experiments in the excited singlet state. Although no obvious fluorescence quenching of ketones could be detected in the presence of amine, the iodonium salt proved to be an excellent fluorescence quencher for the different ketone derivatives. The fluorescence quenching process of ketones by the iodonium salt was conducted and the different spectra are presented in Fig. 7. Both ketone-1 and ketone-2 could emit a strong fluorescence signal in acetonitrile between 450 nm and 650 nm by the same excitation wavelength of 410 nm. However, upon the increasing addition of iodonium salt (Speedcure 938) from 0 M to about 7.5×10^{-3} M, the fluorescence intensity decreased vigorously, implying a clear fluorescence quenching phenomenon for these two ketones (Fig. 7a, 7c). Moreover, based on the Stern–Volmer treatment, a linear relationship could be established between the fluorescence quenching of ketones and the concentration of added iodonium salt. The interaction constant (K_{sv}) for ketone-1/Iod was about 278 M^{-1} , while the K_{sv} for ketone-2/Iod was 208 M^{-1} , which is a little

lower (Fig. 7b, 7d). Further, the electron transfer quantum yields (Φ_{et}) for the fluorescence quenching experiments were calculated according to the following equation:^{32,33}

$$\Phi_{\text{et}} = K_{\text{SV}}[\text{Iod}] / (1 + K_{\text{SV}}[\text{Iod}]) \quad (2)$$

Here, $[\text{Iod}]$ is the concentration of the iodonium salt in the TA resin, *i.e.* 0.043 M.

It turns out that the ketone-1/Iod showed a little higher electron transfer quantum yields ($\Phi_{\text{et, ketone-1/Iod}}$, 0.923) than that of ketone-2/Iod ($\Phi_{\text{et, ketone-2/Iod}}$, 0.899), demonstrating a strong interaction between ketones and the iodonium salt. All the above photolysis and fluorescence quenching characterizations reveal that ketone-1 illustrated a higher photochemical reactivity than ketone-2 in the presence of additives.

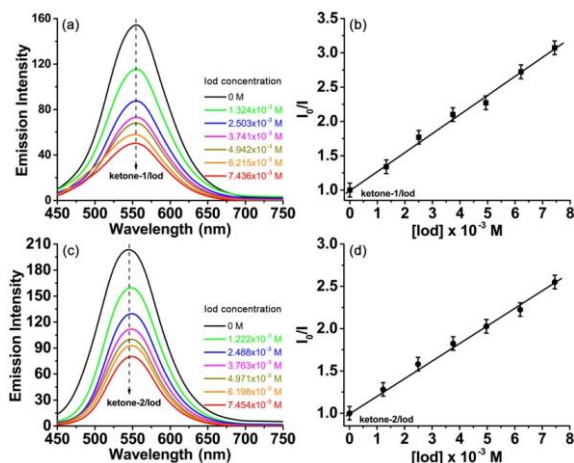


Figure 7. Fluorescence quenching of (a) ketone-1 ($3.96 \times 10^{-5} \text{ M}$) and (c) ketone-2 ($3.55 \times 10^{-5} \text{ M}$) upon the increasing addition of iodonium salt (Speedcure 938) in acetonitrile, $\lambda_{\text{exc}}=410 \text{ nm}$; Stern-Volmer treatment for (b) ketone-1/Iod and (d) ketone-2/Iod, respectively.

3.7. 3D printing experiments through direct laser write

Because ketone-1 showed the highest photoreactivity and initiation ability for the free radical polymerization of acrylates, the ketone-1/amine/Iod three-component system was selected for the 3D printing experiments with TA as the monomer to fabricate 3D patterns. Direct laser write experiments of TA upon laser diode irradiation at 405 nm were performed under air, resulting in efficient free radical polymerization only in the irradiated area. Interestingly, within a very short time ($<1 \text{ min}$ for a 1 cm length pattern) some macroscopic patterns, “CXC” and “WZQ”, were generated with real three-dimensional structures (thickness $>1.5 \text{ mm}$). These obtained patterns were further observed and analyzed by numerical optical microscopy, as shown in Fig. 8. The step width between the photocured and non-cured resin was about $50 \mu\text{m}$, which is in accordance with the spot size of the laser, thus exemplifying an excellent spatial resolution for the products.^{34,35} The 3D printing results of TA induced by ketone-1, in

turn, reflect the high photoinitiation efficiency of ketone derivatives and broaden the potential application prospect.

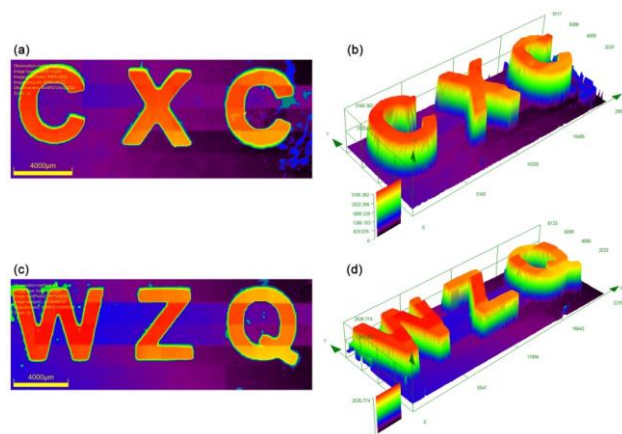


Figure 8. Free radical photopolymerization of TA for 3D printing experiments upon laser diode irradiation at 405 nm with ketone–I/amine/Iod system and characterization of the generated 3D patterns by numerical optical microscopy: (left) top surface morphology and (right) 3D overall appearance in color pattern, respectively. The scale bar is 4000 μm.

3.8. Access to composites

The preparation of fillers contained composites through the photopolymerization approach still remains a big challenge, due to the relevant light penetration issue and internal filter effect.^{36,37} The high photoinitiation ability of the designed ketone derivatives inspired us to investigate the possibility to prepare composites via photopolymerization with ketones-based photoinitiating systems. In this work, the silica fine powder was selected as a benchmark filler and added into TA resin with 20% (w%) weight percent. In the presence of ketone–I/amine/Iod three-component system, finally the depth of cure for TA resin reached over 1.2 mm under the LED@405 nm irradiation for 5 min, as shown in Fig. S5a. Interestingly, the 3D printing technique was applied to the above composite and 3D patterns, *e.g.* “FLY”, could be easily fabricated (Fig. S5b). Further, the numerical optical microscopy observation revealed excellent spatial resolution for the generated patterns, as illustrated in Fig. 9. The depth of cure and laser write experiments demonstrated that the ketone–based systems with high photoinitiation ability could pave the way for the access to thick composites as well as the potential application in 3D printing for reinforced materials.

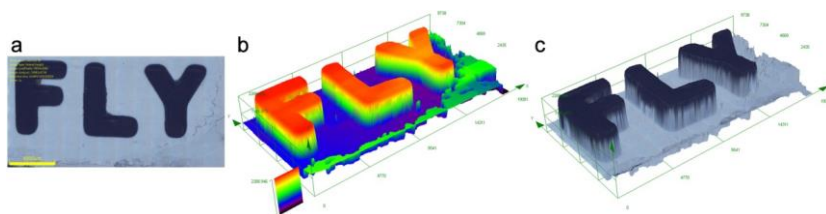


Figure 9. Free radical photopolymerization of TA containing 20% (w%) silica filler for 3D printing experiments upon laser diode irradiation at 405 nm with ketone–I/amine/Iod system and characterization of the generated 3D patterns by numerical optical microscopy: (a) top surface morphology; 3-D overall appearance in (b) color and (c) black-and-white patterns, respectively. The scale bar is 4000 μm .

4. Conclusion

In summary, in this paper, thirteen ketone derivatives containing different central cyclohexanone cores and peripheral substituting moieties were designed and proposed as possible photoinitiators. Through *in silico* design by molecular modeling calculations, ketones never synthesized before were prepared. Noticeably, these ketones have been specifically designed for photopolymerization experiments. In combination with different additives (EDB and Iodonium), the photoinitiation abilities of these ketones for the free radical polymerization and the cationic polymerization upon visible LED@405 nm irradiation were systematically studied and compared through real time Fourier transform infrared spectroscopy. Ketone–1 proved to be the most efficient one for both free radical polymerization of acrylates and cationic polymerization of epoxides. The photochemical mechanism for the ketone/amine/Iod three–component systems was thoroughly investigated by steady state photolysis and excited state fluorescence quenching experiments. Further, the high photoinitiation efficiency of ketone–1 found huge application prospect in 3D printing experiments to produce tridimensional patterns. Besides, thick photocomposites containing fillers were also successfully prepared in the presence of ketone–1 under LED irradiation.

Acknowledgments

Yangyang Xu thanks the financial support from the Anhui Provincial Natural Science Foundation (1808085QB42) and China Scholarship Council (CSC). Pu Xiao acknowledges funding from the Australian Research Council (FT170100301). This work was granted access to the HPC resources of the Mesocentre of the University of Strasbourg.

References

1. Y. Yagci, S. Jockusch and N. J. Turro, *Macromolecules*, 2010, **43**, 6245–6260.
2. F. Dumur, D. Gigmes, J.-P. Fouassier and J. Lalevée, *Acc. Chem. Res.*, 2016, **49**, 1980–1989.
3. H. Lai, J. Zhang, F. Xing and P. Xiao, *Chem. Soc. Rev.*, 2020, **49**, 1867–1886.
4. B. P. Fors and C. J. Hawker, *Angew. Chem. Int. Ed.*, 2012, **51**, 8850–8853.

5. N. Corrigan, S. Shanmugam, J. Xu and C. Boyer, *Chem. Soc. Rev.*, 2016, **45**, 6165–6212.
6. C. Dietlin, S. Schweizer, P. Xiao, J. Zhang, F. Morlet-Savary, B. Graff, J.-P. Fouassier and J. Lalevée, *Polym. Chem.*, 2015, **6**, 3895–3912.
7. A. J. Perkowski, W. You and D. A. Nicewicz, *J. Am. Chem. Soc.*, 2015, **137**, 7580–7583.
8. K. Tu, T. Xu, L. Zhang, Z. Cheng and X. Zhu, *RSC Adv.*, 2017, **7**, 24040–24045.
9. W. Qiu, M. Li, Y. Yang, Z. Li and K. Dietliker, *Polym. Chem.*, 2020, **11**, 1356–1363.
10. Y.-H. Li and Y.-C. Chen, *Polym. Chem.*, 2020, **11**, 1504–1513.
11. J. Yu, Y. Gao, S. Jiang and F. Sun, *Macromolecules*, 2019, **52**, 1707–1717.
12. Z. Li, W. Shen, X. Liu and R. Liu, *Polym. Chem.*, 2017, **8**, 1579–1588.
13. Z. Li, X. Zou, G. Zhu, X. Liu and R. Liu, *ACS Appl. Mater. Interfaces*, 2018, **10**, 16113–16123.
14. Z. Liu, M. Zhang, B. Bhandari, Y. Wang, *Trends Food Sci. Tech.*, 2017, **69**, 83–94.
15. L. Tang, J. Nie and X. Zhu, *Polym. Chem.*, 2020, **11**, 2855–2863.
16. J. Li, Y. Hao, M. Zhong, L. Tang, J. Nie, X. Zhu, *Dyes Pigments*, 2019, **165**, 467–473.
17. A. Bagheri and J. Jin, *ACS Appl. Polym. Mater.*, 2019, **1**, 593–611.
18. Y. Xu, C. Jambou, K. Sun, J. Lalevée, A. Simon-Masseron and P. Xiao, *ACS Appl. Polym. Mater.*, 2019, **1**, 2854–2861.
19. Y.-Y. Xu, Z.-F. Ding, F.-Y. Liu, K. Sun, C. Dietlin, J. Lalevée and P. Xiao, *ACS Appl. Mater. Interfaces*, 2020, **12**, 1658–1664.
20. K. Sun, Y. Xu, F. Dumur, F. Morlet-Savary, H. Chen, C. Dietlin, B. Graff, J. Lalevée and P. Xiao, *Polym. Chem.*, 2020, **11**, 2230–2242.
21. B. Graff, J. E. Klee, C. Fik, M. Maier, J. P. Fouassier and J. Lalevée, *Macromol. Rapid Commun.*, 2017, **38**, 1600470.
22. Y. Xu, G. Noirbent, D. Brunel, F. Liu, D. Gigmes, K. Sun, Y. Zhang, S. Liu, F. Morlet-Savary, P. Xiao, F. Dumur and J. Lalevée, *Eur. Polym. J.*, 2020, **132**, 109737.
23. H. Mokbel, D. Anderson, R. Plenderleith, C. Dietlin, F. Morlet-Savary, F. Dumur, D. Gigmes, J. P. Fouassier and J. Lalevée, *Prog. Org. Coat.*, 2019, **132**, 50–61.
24. A. Baralle, P. Garra, B. Graff, F. Morlet-Savary, C. Dietlin, J. P. Fouassier, S. Lakhdar and J. Lalevée, *Macromolecules*, 2019, **52**, 3448–3453.
25. Y. Xu, G. Noirbent, D. Brunel, Z. Ding, D. Gigmes, B. Graff, P. Xiao, F. Dumur and J. Lalevée, *Polym. Chem.*, 2020, **XX-XX (accepted)**.
26. A. A. Mousawi, F. Dumur, P. Garra, J. Toufaily, T. Hamieh, B. Graff, D. Gigmes, J. P. Fouassier and J. Lalevée, *Macromolecules*, 2017, **50**, 2747–2758.
27. M. Abdallah, A. Hijazi, B. Graff, J.-P. Fouassier, F. Dumur and J. Lalevée, *J. Photoch. Photobio. A*, 2020, **400**, 112698.
28. M. Rahal, M. Abdallah, T.-T. Bui, F. Goubard, B. Graff, F. Dumur, J. Toufaily, T. Hamieh and J. Lalevée, *Polym. Chem.*, 2020, **11**, 3349–3359.
29. A. A. Mousawi, P. Garra, X. Sallenave, F. Dumur, J. Toufaily, T. Hamieh, B. Graff, D. Gigmes, J. P. Fouassier and J. Lalevée, *Macromolecules*, 2018, **51**, 1811–1821.

Commenté [JL1]: update

30. A. A. Mousawi, P. Garra, M. Schmitt, J. Toufaily, T. Hamieh, B. Graff, J. P. Fouassier, F. Dumur and J. Lalevée, *Macromolecules*, 2018, **51**, 4633–4641.
31. A. A. Mousawi, C. Poriol, F. Dumur, J. Toufaily, T. Hamieh, J. P. Fouassier and J. Lalevée, *Macromolecules*, 2017, **50**, 746–753.
32. E. Hola, J. Ortyl, M. Jankowska, M. Pilch, M. Galek, F. Morlet-Savary, B. Graff, C. Dietlin and J. Lalevée, *Polym. Chem.*, 2020, **11**, 922–935.
33. S. Liu, D. Brunel, K. Sun, Y. Xu, F. Morlet-Savary, B. Graff, P. Xiao, F. Dumur and J. Lalevée, *Polym. Chem.*, 2020, **11**, 3551–3556.
34. M. Abdallah, A. Hijazi, J.-T. Lin, B. Graff, F. Dumur and J. Lalevée, *ACS Appl. Polym. Mater.*, 2020, **2**, 2769–2780.
35. M. Abdallah, A. Hijazi, B. Graff, J.-P. Fouassier, G. Rodeghiero, A. Gualandi, F. Dumur, P. G. Cozzi and J. Lalevée, *Polym. Chem.*, 2019, **10**, 872–884.
36. J. H. Lee, R. K. Prud'homme and I. A. Aksay, *J. Mater. Res.*, 2001, **16**, 3536–3544.
37. P. Garra, C. Dietlin, F. Morlet-Savary, F. Dumur, D. Gigmes, J.-P. Fouassier and J. Lalevée, *Polym. Chem.*, 2017, **8**, 7088–7101.

Supporting Information

Design of ketone derivatives as highly efficient photoinitiators for free radical and cationic photopolymerizations and application in 3D printing

Yangyang Xu,^{a,b,c*} Zhaofu Ding,^a Haibin Zhu,^a Bernadette Graff,^{b,c} Pu Xiao,^{d*} Frédéric Dumur^{e*} and Jacques Lalevée^{b,c*}

^aCollege of Chemistry and Materials Science, Anhui Normal University, South Jiuhua Road 189, Wuhu 241002, China. E-mail: ahnuxyy@ahnu.edu.cn

^bUniversité de Haute-Alsace, CNRS, IS2M UMR 7361, F-68100 Mulhouse, France. E-mail: jacques.lalevee@uha.fr

^cUniversité de Strasbourg, France.

^dResearch School of Chemistry, Australian National University, Canberra, ACT 2601, Australia. E-mail: pu.xiao@anu.edu.au

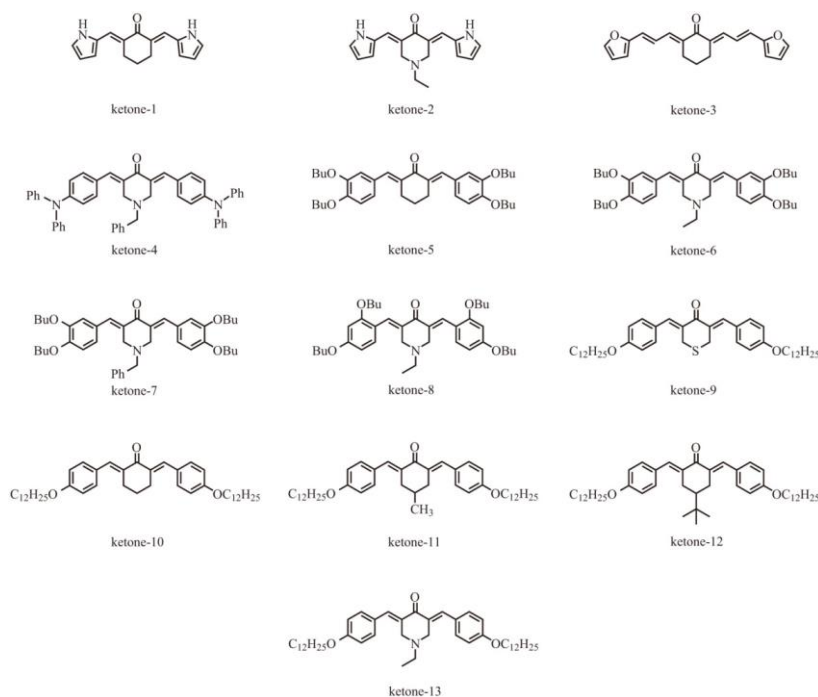
^eAix Marseille Univ, CNRS, ICR UMR 7273, F-13397 Marseille, France. E-mail: Frederic.dumur@univ-amu.fr

Index

- (1) Synthesis of ketones.
- (2) Formulation preparation.
- (3) DFT calculation.
- (4) Photopolymerization profiles.
- (5) IR spectra.
- (6) Photolysis experiments.
- (7) Photocomposite preparation.

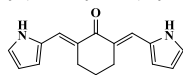
Synthesis of ketone-1~ketone-13

All reagents and solvents were purchased from Aldrich, TCI, Fluorochem or Alfa Aesar and used as received without further purification. Mass spectroscopy was performed by the Spectropole of Aix-Marseille University. ESI mass spectral analyses were recorded with a 3200 QTRAP (Applied Biosystems SCIEX) mass spectrometer. The HRMS mass spectral analysis was performed with a QStar Elite (Applied Biosystems SCIEX) mass spectrometer. Elemental analyses were recorded with a Thermo Finnigan EA 1112 elemental analysis apparatus driven by the Eager 300 software. ^1H and ^{13}C NMR spectra were determined at room temperature in 5 mm o.d. tubes on a Bruker Avance 400 spectrometer of the Spectropole: ^1H (400 MHz) and ^{13}C (100 MHz). The ^1H chemical shifts were referenced to the solvent peaks: DMSO (2.49 ppm), CDCl_3 (7.26 ppm) and the ^{13}C chemical shifts were referenced to the solvent peaks: DMSO (49.5 ppm), CDCl_3 (77.0 ppm), respectively. All photoinitiators were prepared with analytical purity up to accepted standards for new organic compounds (>98%), which were checked by high field NMR analysis.



Scheme S1. Chemical structures of ketone-1~ketone-13.

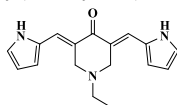
Synthesis of 2,6-bis((1*H*-pyrrol-2-yl)methylene)cyclohexan-1-one (ketone-1)



Chemical Formula: C₁₆H₁₆N₂O
Molecular Weight: 252.3170

Cyclohexanone (0.98 g, 10 mmol, M = 98.14 g/mol) and pyrrole-2-carboxaldehyde (1.90 g, 20 mmol, M = 95.10 g/mol) were dissolved in ethanol (50 mL) and aq. KOH (40%) (15 mL) was added. The solution was stirred at room temperature overnight. During reaction, a precipitate formed. It was filtered off, washed several times with ethanol and dried under vacuum. The resulting solid was dissolved in dichloromethane and the solution was filtered on a plug of SiO₂ using dichloromethane as the eluent. The solvent was removed under reduced pressure. Dissolution in a minimum of dichloromethane followed by addition of pentane precipitated a solid that was filtered off, washed several times with pentane and dried under vacuum (2.32 g, 92% yield). ¹H NMR (300 MHz, DMSO-d₆) δ: 1.78-1.81 (m, 2H), 2.75-2.77 (m, 4H), 6.25-6.26 (t, 2H, J = 2.9 Hz), 6.52 (d, 2H, J = 3.3 Hz), 7.05 (d, 2H, J = 1.3 Hz), 7.60 (s, 2H); ¹³C NMR (75 MHz, DMSO-d₆) δ: 21.6, 27.8, 110.8, 113.2, 122.2, 126.0, 129.1, 129.3, 186.9; HRMS (ESI MS) m/z: theor: 253.1335 found: 253.1332 ([M+H]⁺ detected).

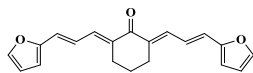
Synthesis of 3,5-bis((1*H*-pyrrol-2-yl)methylene)-1-ethylpiperidin-4-one (ketone-2)



Chemical Formula: C₁₇H₁₉N₃O
Molecular Weight: 281.3590

1-Ethylpiperidin-4-one (1.27 g, 10 mmol, M = 127.19 g/mol) and pyrrole-2-carboxaldehyde (1.90 g, 20 mmol, M = 95.10 g/mol) were dissolved in ethanol (50 mL) and aq. KOH (40%) (15 mL) was added. The solution was stirred at room temperature overnight. During reaction, a precipitate formed. It was filtered off, washed several times with ethanol and dried under vacuum. The resulting solid was dissolved in dichloromethane and the solution was filtered on a plug of SiO₂ using dichloromethane as the eluent. The solvent was removed under reduced pressure. Dissolution in a minimum of dichloromethane followed by addition of pentane precipitated a solid that was filtered off, washed several times with pentane and dried under vacuum (2.67 g, 95% yield). ¹H NMR (300 MHz, CDCl₃) δ: 1.19 (t, 3H, J = 7.1 Hz), 2.72 (q, 2H, J = 7.1 Hz), 3.81 (s, 4H), 6.37-6.39 (m, 2H), 6.50-6.51 (m, 2H), 7.01-7.02 (m, 2H), 7.72 (s, 2H), 8.99 (brs, 2H); ¹H NMR (300 MHz, DMSO-d₆) δ: 1.10 (t, 3H, J = 7.1 Hz), 2.65 (q, 2H, J = 7.1 Hz), 3.65 (s, 4H), 6.28-6.30 (m, 2H), 6.54 (s, 2H), 7.10 (s, 2H), 7.55 (s, 2H); ¹³C NMR (75 MHz, DMSO-d₆) δ: 12.3, 50.9, 53.8, 111.1, 113.5, 122.6, 124.2, 127.2, 128.2, 184.9; HRMS (ESI MS) m/z: theor: 282.1601 found: 282.1600 ([M+H]⁺ detected).

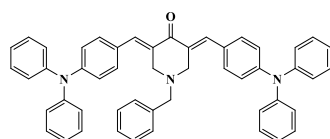
Synthesis of 2,6-bis((*E*)-3-(furan-2-yl)allylidene)cyclohexan-1-one (ketone-3)



Chemical Formula: C₂₀H₁₈O₃
Molecular Weight: 306.3610

Cyclohexanone (0.98 g, 10 mmol, M = 98.14 g/mol) and *trans*-3-(2-furyl)acrolein (2.44 g, 20 mmol, M = 122.12 g/mol) were dissolved in ethanol (50 mL) and aq. KOH (40%) (15 mL) was added. The solution was stirred at room temperature overnight. During reaction, a precipitate formed. It was filtered off, washed several times with ethanol and dried under vacuum. The resulting solid was dissolved in dichloromethane and the solution was filtered on a plug of SiO₂ using dichloromethane as the eluent. The solvent was removed under reduced pressure. Dissolution in a minimum of dichloromethane followed by addition of pentane precipitated a solid that was filtered off, washed several times with pentane and dried under vacuum (2.45 g, 80% yield). ¹H NMR (300 MHz, CDCl₃) δ: 1.83-1.89 (m, 2H), 2.75-2.79 (m, 4H), 6.43-6.45 (m, 4H), 6.73 (d, 2H, J = 15.2 Hz), 6.95 (dd, 2H, J = 15.2 Hz, J = 12.0 Hz), 7.41 (d, 2H, J = 12.0 Hz), 7.43 (s, 2H); ¹³C NMR (75 MHz, DMSO-d₆) δ: 22.0, 26.6, 11.6, 112.2, 122.2, 127.0, 135.6, 135.9, 143.5, 153.0, 188.7; HRMS (ESI MS) m/z: theor: 307.1329 found: 307.1330 ([M+H]⁺ detected).

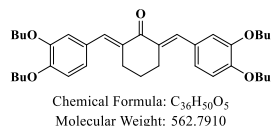
Synthesis of 1-benzyl-3,5-bis((*E*)-4-(diphenylamino)benzylidene)piperidin-4-one (ketone-4)



Chemical Formula: C₅₀H₄₁N₃O
Molecular Weight: 699.8980

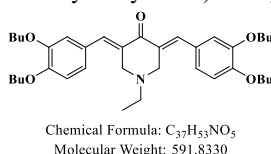
1-Benzylpiperidin-4-one (1.90 g, 10 mmol, M = 189.26 g/mol) and 4-(diphenylamino)benzaldehyde (5.47 g, 20 mmol, M = 273.33 g/mol) were dissolved in ethanol (50 mL) and aq. KOH (40%) (15 mL) was added. The solution was stirred at room temperature overnight. During reaction, a precipitate formed. It was filtered off, washed several times with ethanol and dried under vacuum. The resulting solid was dissolved in dichloromethane and the solution was filtered on a plug of SiO₂ using dichloromethane as the eluent. The solvent was removed under reduced pressure. Dissolution in a minimum of dichloromethane followed by addition of pentane precipitated a solid that was filtered off, washed several times with pentane and dried under vacuum (6.23 g, 89% yield). ¹H NMR (300 MHz, CDCl₃) δ: 3.74 (m, 2H), 3.87 (m, 4H), 7.02 (d, 4H, J = 8.6 Hz), 7.09-7.15 (m, 12H), 7.23-7.34 (m, 19H); ¹³C NMR (75 MHz, CDCl₃) δ: 54.6, 121.6, 123.9, 125.2, 125.3, 127.2, 128.3, 128.6, 129.1, 129.3, 129.5, 131.5, 131.8, 136.0, 137.6, 147.0, 148.6, 187.5; HRMS (ESI MS) m/z: theor: 700.3322 found: 700.3324 ([M+H]⁺ detected).

Synthesis of 2,6-bis((*E*)-3,4-dibutoxybenzylidene)cyclohexan-1-one (ketone-5)



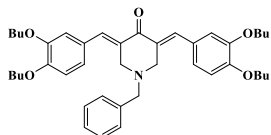
Cyclohexanone (0.98 g, 10 mmol, $M = 98.14$ g/mol) and 3,4-dibutoxybenzaldehyde (5.00 g, 20 mmol, $M = 250.34$ g/mol) were dissolved in ethanol (50 mL) and aq. KOH (40%) (15 mL) was added. The solution was stirred at room temperature overnight. During reaction, a precipitate formed. It was filtered off, washed several times with ethanol and dried under vacuum. The resulting solid was dissolved in dichloromethane and the solution was filtered on a plug of SiO_2 using dichloromethane as the eluent. The solvent was removed under reduced pressure. Dissolution in a minimum of dichloromethane followed by addition of pentane precipitated a solid that was filtered off, washed several times with pentane and dried under vacuum (4.89 g, 87% yield). 1H NMR (300 MHz, $CDCl_3$) δ : 0.99 (t, 6H, $J = 7.4$ Hz), 1.00 (t, 6H, $J = 7.4$ Hz), 1.47-1.57 (m, 8H), 1.78-1.85 (m, 10H), 2.93-2.94 (m, 4H), 4.03 (t, 4H, $J = 7.4$ Hz), 4.04 (t, 4H, $J = 7.4$ Hz), 6.89 (d, 2H, $J = 8.4$ Hz), 7.03 (d, 2H, $J = 1.9$ Hz), 7.07 (dd, 2H, $J = 8.4$ Hz, $J = 1.9$ Hz), 7.73 (s, 2H); ^{13}C NMR (75 MHz, $CDCl_3$) δ : 13.8, 13.9, 19.2, 19.3, 23.1, 28.5, 31.3, 31.4, 68.8, 69.2, 113.1, 116.6, 124.2, 129.0, 134.3, 136.9, 148.7, 150.0, 190.1; HRMS (ESI MS) m/z : theor: 563.3731 found: 563.3736 ($[M+H]^+$ detected).

Synthesis of 3,5-bis((*E*)-3,4-dibutoxybenzylidene)-1-ethylpiperidin-4-one (ketone-6)



1-Ethylpiperidin-4-one (1.27 g, 10 mmol, $M = 127.19$ g/mol) and 3,4-dibutoxybenzaldehyde (5.00 g, 20 mmol, $M = 250.34$ g/mol) were dissolved in ethanol (50 mL) and aq. KOH (40%) (15 mL) was added. The solution was stirred at room temperature overnight. During reaction, a precipitate formed. It was filtered off, washed several times with ethanol and dried under vacuum. The resulting solid was dissolved in dichloromethane and the solution was filtered on a plug of SiO_2 using dichloromethane as the eluent. The solvent was removed under reduced pressure. Dissolution in a minimum of dichloromethane followed by addition of pentane precipitated a solid that was filtered off, washed several times with pentane and dried under vacuum (4.96 g, 84% yield). 1H NMR (300 MHz, $CDCl_3$) δ : 0.99 (t, 6H, $J = 7.4$ Hz), 1.00 (t, 6H, $J = 7.4$ Hz), 1.08 (t, 3H, $J = 7.1$ Hz), 1.47-1.57 (m, 8H), 1.78-1.86 (m, 8H), 2.63 (q, 2H, $J = 7.1$ Hz), 3.85 (s, 4H), 4.03 (t, 4H, $J = 6.7$ Hz), 4.05 (t, 4H, $J = 6.7$ Hz), 6.89-7.00 (m, 6H), 7.75 (s, 2H); ^{13}C NMR (75 MHz, $CDCl_3$) δ : 12.5, 13.8, 13.9, 19.2, 31.2, 31.3, 68.8, 69.2, 113.0, 116.5, 124.2, 128.3, 131.4, 136.6, 148.7, 150.3, 187.2; HRMS (ESI MS) m/z : theor: 592.3997 found: 593.3995 ($[M+H]^+$ detected).

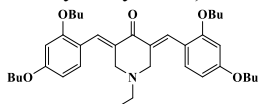
Synthesis of 1-benzyl-3,5-bis((*E*)-3,4-dibutoxybenzylidene)piperidin-4-one (ketone-7)



Chemical Formula: $C_{42}H_{55}NO_5$
Molecular Weight: 653.9040

1-Benzylpiperidin-4-one (1.90 g, 10 mmol, $M = 189.26$ g/mol) and 3,4-dibutoxybenzaldehyde (5.00 g, 20 mmol, $M = 250.34$ g/mol) were dissolved in ethanol (50 mL) and aq. KOH (40%) (15 mL) was added. The solution was stirred at room temperature overnight. During reaction, a precipitate formed. It was filtered off, washed several times with ethanol and dried under vacuum. The resulting solid was dissolved in dichloromethane and the solution was filtered on a plug of SiO_2 using dichloromethane as the eluent. The solvent was removed under reduced pressure. Dissolution in a minimum of dichloromethane followed by addition of pentane precipitated a solid that was filtered off, washed several times with pentane and dried under vacuum (5.55 g, 85% yield). 1H NMR (300 MHz, $CDCl_3$) δ : 0.99 (t, 6H, $J = 7.4$ Hz), 1.00 (t, 6H, $J = 7.4$ Hz), 1.43-1.56 (m, 8H), 1.77-1.87 (m, 8H), 3.73 (s, 2H), 3.86 (s, 4H), 3.97 (t, 4H, $J = 6.5$ Hz), 4.03 (t, 4H, $J = 6.5$ Hz), 6.85-6.95 (m, 6H), 7.18-7.28 (m, 5H), 7.73 (s, 2H); ^{13}C NMR (75 MHz, $CDCl_3$) δ : 13.8, 13.9, 19.2, 19.3, 31.2, 31.3, 54.5, 61.7, 68.8, 69.0, 113.0, 116.1, 124.5, 127.4, 128.2, 128.3, 129.0, 131.4, 136.4, 137.4, 148.7, 150.2, 187.4; HRMS (ESI MS) m/z : theor: 654.4153 found: 654.5155 ($[M+H]^+$ detected).

Synthesis of 3,5-bis((*E*)-2,4-dibutoxybenzylidene)-1-ethylpiperidin-4-one (ketone-8)

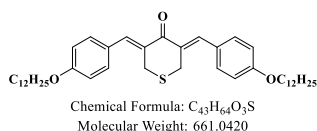


Chemical Formula: $C_{37}H_{53}NO_5$
Molecular Weight: 591.8330

1-Ethylpiperidin-4-one (1.27 g, 10 mmol, $M = 127.19$ g/mol) and 2,4-dibutoxybenzaldehyde (5.00 g, 20 mmol, $M = 250.34$ g/mol) were dissolved in ethanol (50 mL) and aq. KOH (40%) (15 mL) was added. The solution was stirred at room temperature overnight. During reaction, a precipitate formed. It was filtered off, washed several times with ethanol and dried under vacuum. The resulting solid was dissolved in dichloromethane and the solution was filtered on a plug of SiO_2 using dichloromethane as the eluent. The solvent was removed under reduced pressure. Dissolution in a minimum of dichloromethane followed by addition of pentane precipitated a solid that was filtered off, washed several times with pentane and dried under vacuum (4.61 g, 78% yield). 1H NMR (300 MHz, $CDCl_3$) δ : 0.97 (t, 6H, $J = 7.4$ Hz), 0.98 (t, 6H, $J = 7.4$ Hz), 1.02 (t, 3H, $J = 7.2$ Hz), 1.43-1.56 (m, 8H), 1.73-1.87 (m, 8H), 2.57 (q, 2H, $J = 7.2$ Hz), 3.77 (brs, 4H), 3.97 (t, 4H, $J = 6.5$ Hz), 3.99 (q, 4H, $J = 6.5$ Hz), 6.46-6.50 (m, 4H), 7.13 (d, 2H, $J = 8.1$ Hz), 8.09 (s, 2H); ^{13}C NMR (75 MHz, $CDCl_3$) δ : 12.5, 13.8, 19.2, 19.3, 31.2, 31.3, 54.8, 67.8, 68.2, 99.6, 104.8, 117.6, 131.3, 159.7, 161.4, 187.1; HRMS (ESI MS) m/z : theor: 592.3997 found: 592.3999 ($[M+H]^+$ detected).

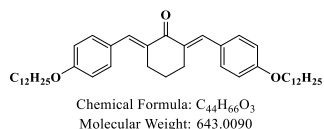
detected).

Synthesis of 3,5-bis((*Z*)-4-(dodecyloxy)benzylidene)tetrahydro-4*H*-thiopyran-4-one (ketone-9)



Tetrahydro-4*H*-thiopyran-4-one (1.17 g, 10 mmol, M = 116.18 g/mol) and 4-(dodecyloxy)benzaldehyde (5.77 g, 20 mmol, M = 288.47 g/mol) were dissolved in ethanol (50 mL) and aq. KOH (40%) (15 mL) was added. The solution was stirred at room temperature overnight. During reaction, a precipitate formed. It was filtered off, washed several times with ethanol and dried under vacuum. The resulting solid was dissolved in dichloromethane and the solution was filtered on a plug of SiO₂ using dichloromethane as the eluent. The solvent was removed under reduced pressure. Dissolution in a minimum of dichloromethane followed by addition of pentane precipitated a solid that was filtered off, washed several times with pentane and dried under vacuum (5.42 g, 82% yield). ¹H NMR (300 MHz, CDCl₃) δ: 0.88 (t, 6H, J = 6.6 Hz), 1.27-1.40 (m, 36H), 1.46 (qt, 4H, J = 6.2 Hz), 1.80 (qt, 4H, J = 6.6 Hz), 3.93 (s, 4H), 3.99 (q, 4H, J = 6.6 Hz), 6.93 (d, 4H, J = 8.8 Hz), 7.37 (d, 4H, J = 8.8 Hz), 7.74 (s, 2H); ¹³C NMR (75 MHz, CDCl₃) δ: 14.1, 22.7, 26.0, 29.2, 29.34, 29.37, 29.56, 29.58, 29.62, 29.65, 30.2, 31.9, 68.2, 114.6, 127.6, 132.0, 136.7, 159.9, 188.9; HRMS (ESI MS) m/z: theor: 661.4649 found: 661.4644 ([M+H]⁺ detected).

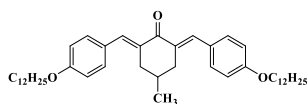
Synthesis of 2,6-bis((*E*)-4-(dodecyloxy)benzylidene)cyclohexan-1-one (ketone 10)



Cyclohexanone (0.98 g, 10 mmol, M = 98.14 g/mol) and 4-(dodecyloxy)benzaldehyde (5.77 g, 20 mmol, M = 288.47 g/mol) were dissolved in ethanol (50 mL) and aq. KOH (40%) (15 mL) was added. The solution was stirred at room temperature overnight. During reaction, a precipitate formed. It was filtered off, washed several times with ethanol and dried under vacuum. The resulting solid was dissolved in dichloromethane and the solution was filtered on a plug of SiO₂ using dichloromethane as the eluent. The solvent was removed under reduced pressure. Dissolution in a minimum of dichloromethane followed by addition of pentane precipitated a solid that was filtered off, washed several times with pentane and dried under vacuum (5.78 g, 88% yield). ¹H NMR (300 MHz, CDCl₃) δ: 0.88 (t, 6H, J = 6.5 Hz), 1.25-1.40 (m, 36H), 1.46 (qt, 4H, J = 7.6 Hz), 1.80 (qt, 4H, J = 8.1 Hz), 2.90-2.94 (m, 4H), 3.99 (t, 4H, J = 6.5 Hz), 6.92 (d, 4H, J = 8.8 Hz), 7.44 (d, 4H, J = 8.8 Hz), 7.76 (s, 2H); ¹³C NMR (75 MHz, CDCl₃) δ: 14.1, 22.7, 23.1, 26.0, 28.5, 29.2, 29.3, 29.4, 29.60, 29.63, 29.66, 31.9, 114.4, 128.5,

132.2, 134.2, 136.6, 159.5, 190.2; HRMS (ESI MS) m/z : theor: 643.5085 found: 643.5088 ($[M+H]^+$ detected).

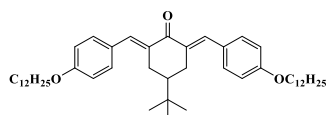
Synthesis of 2,6-bis((*E*)-4-(dodecyloxy)benzylidene)-4-methylcyclohexan-1-one (ketone-11)



Chemical Formula: $C_{45}H_{68}O_3$
Molecular Weight: 657.0360

4-Methylcyclohexan-1-one (1.12 g, 10 mmol, $M = 112.17$ g/mol) and 4-(dodecyloxy)benzaldehyde (5.77 g, 20 mmol, $M = 288.47$ g/mol) were dissolved in ethanol (50 mL) and aq. KOH (40%) (15 mL) was added. The solution was stirred at room temperature overnight. During reaction, a precipitate formed. It was filtered off, washed several times with ethanol and dried under vacuum. The resulting solid was dissolved in dichloromethane and the solution was filtered on a plug of SiO_2 using dichloromethane as the eluent. The solvent was removed under reduced pressure. Dissolution in a minimum of dichloromethane followed by addition of pentane precipitated a solid that was filtered off, washed several times with pentane and dried under vacuum (5.98 g, 91% yield). 1H NMR (300 MHz, $CDCl_3$) δ : 0.89 (t, 6H, $J = 6.6$ Hz), 1.09 (d, 3H, $J = 6.5$ Hz), 1.25-1.40 (m, 36H), 1.46 (qt, 4H, $J = 7.9$ Hz), 1.80 (qt, 4H, $J = 7.9$ Hz), 1.87-1.92 (m, 1H), 2.46-2.53 (m, 2H), 3.05 (dd, 2H, $J = 15.7$ Hz, $J = 3.5$ Hz), 3.99 (t, 4H, $J = 6.7$ Hz), 6.92 (d, 4H, $J = 8.8$ Hz), 7.44 (d, 4H, $J = 8.8$ Hz), 7.76 (s, 2H); ^{13}C NMR (75 MHz, $CDCl_3$) δ : 14.1, 21.7, 22.7, 26.0, 29.2, 29.3, 29.38, 29.42, 29.57, 29.59, 29.63, 29.65, 31.9, 36.6, 68.1, 114.4, 128.5, 132.2, 133.4, 136.8, 159.6, 190.0; HRMS (ESI MS) m/z : theor: 657.5241 found: 657.5243 ($[M+H]^+$ detected).

Synthesis of 4-(*tert*-butyl)-2,6-bis((*E*)-4-(dodecyloxy)benzylidene)cyclohexan-1-one (ketone-12)

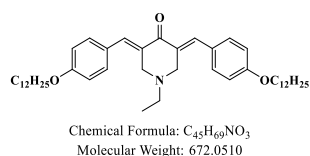


Chemical Formula: $C_{48}H_{74}O_3$
Molecular Weight: 699.1170

4-(*Tert*-butyl)cyclohexan-1-one (1.54 g, 10 mmol, $M = 154.25$ g/mol) and 4-(dodecyloxy)benzaldehyde (5.77 g, 20 mmol, $M = 288.47$ g/mol) were dissolved in ethanol (50 mL) and aq. KOH (40%) (15 mL) was added. The solution was stirred at room temperature overnight. During reaction, a precipitate formed. It was filtered off, washed several times with ethanol and dried under vacuum. The resulting solid was dissolved in dichloromethane and the solution was filtered on a plug of SiO_2 using dichloromethane as the eluent. The solvent was removed under reduced pressure. Dissolution in a minimum of dichloromethane followed by addition of pentane precipitated a solid that was filtered off, washed several times with pentane and dried

under vacuum (6.18 g, 92% yield). ^1H NMR (300 MHz, CDCl_3) δ : 0.89 (t, 6H, $J = 6.7$ Hz), 1.27-1.43 (m, 36H), 1.43-1.48 (m, 4H), 1.80 (qt, 4H, $J = 6.6$ Hz), 2.40-2.47 (m, 2H), 3.15 (dd, 2H, $J = 15.4$ Hz, $J = 1.6$ Hz), 4.00 (t, 4H, $J = 6.6$ Hz), 6.93 (d, 4H, $J = 8.8$ Hz), 7.44 (d, 4H, $J = 8.8$ Hz), 7.73 (d, 2H, $J = 2.3$ Hz); ^{13}C NMR (75 MHz, CDCl_3) δ : 14.1, 22.7, 26.0, 27.4, 29.3, 29.4, 29.57, 29.59, 29.63, 29.66, 31.9, 32.5, 44.4, 68.1, 114.5, 128.6, 132.2, 1134.2, 136.5, 159.5, 190.5; HRMS (ESI MS) m/z : theor: 699.5711 found: 699.5705 ($[\text{M}+\text{H}]^+$ detected).

Synthesis of 3,5-bis((*E*)-4-(dodecyloxy)benzylidene)-1-ethylpiperidin-4-one (ketone-13)



4-(*Tert*-butyl)cyclohexan-1-one (1.27 g, 10 mmol, $M = 127.19$ g/mol) and 4-(dodecyloxy)benzaldehyde (5.77 g, 20 mmol, $M = 288.47$ g/mol) were dissolved in ethanol (50 mL) and aq. KOH (40%) (15 mL) was added. The solution was stirred at room temperature overnight. During reaction, a precipitate formed. It was filtered off, washed several times with ethanol and dried under vacuum. The resulting solid was dissolved in dichloromethane and the solution was filtered on a plug of SiO_2 using dichloromethane as the eluent. The solvent was removed under reduced pressure. Dissolution in a minimum of dichloromethane followed by addition of pentane precipitated a solid that was filtered off, washed several times with pentane and dried under vacuum (5.71 g, 85% yield). ^1H NMR (300 MHz, CDCl_3) δ : 0.88 (t, 6H, $J = 6.6$ Hz), 1.09 (t, 3H, $J = 7.1$ Hz), 1.25-1.40 (m, 36H), 1.46 (qt, 4H, $J = 7.3$ Hz), 1.80 (qt, 4H, $J = 7.0$ Hz), 2.67 (brs, 2H), 3.88 (brs, 2H), 4.00 (t, 4H, $J = 6.5$ Hz), 6.94 (d, 4H, $J = 8.8$ Hz), 7.36 (d, 4H, $J = 8.8$ Hz), 7.81 (brs, 2H); ^{13}C NMR (75 MHz, CDCl_3) δ : 14.1, 22.7, 26.0, 29.2, 29.3, 29.4, 29.57, 29.59, 29.63, 29.66, 31.9, 31.9, 68.2, 114.7, 131.4; HRMS (ESI MS) m/z : theor: 672.5350 found: 672.5353 ($[\text{M}+\text{H}]^+$ detected).

Table S1. Basic formulation for free radical polymerization and cationic polymerization, respectively.

	ketone	amine	Iod	benchmark monomer
free radical polymerization	2.0 mg (0.1%)	40 mg (2%)	40 mg (2%)	2.0 g (TA)
cationic polymerization	2.0 mg (0.1%)	0	40 mg (2%)	2.0 g (EPOX)

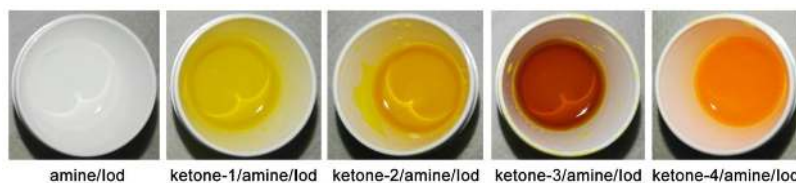


Figure S1. *In-situ* photographs for TA in the presence of different ketone/amine/Iod (0.1/2%/2%, w/w/w) photoinitiating systems, respectively. The first one is a control sample containing amine/Iod (2%/2%, w/w) two-component system in the absence of any ketones.

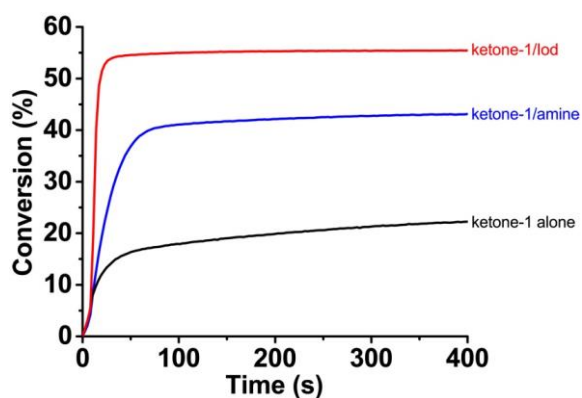


Figure S2. Photopolymerization profiles of TA (C=C conversion vs. irradiation time) upon LED@405 nm irradiation in thin films condition (25 μm) in the presence of ketone-1 alone (black, 0.1%, w) without any additives, ketone-1/amine (blue, 0.1%/2%, w/w) and ketone-1/Iod (red, 0.1%/2%, w/w), respectively.

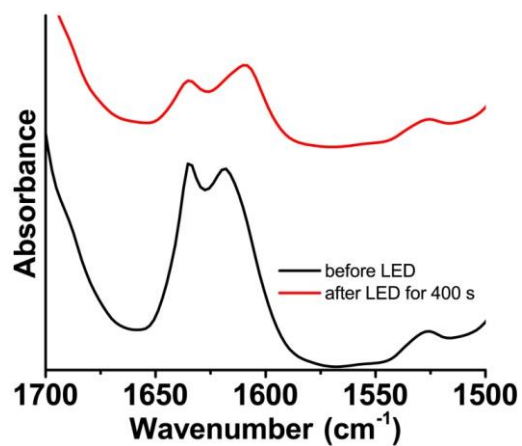


Figure S3. *In-situ* IR spectra recorded for TA in the presence of ketone-1/amine/Iod (0.1/2%/2%, w/w/w) three-component photoinitiating system in thin films condition (25 μm): (black) before and (red) after the irradiation of LED@405 nm for 400 s, respectively.

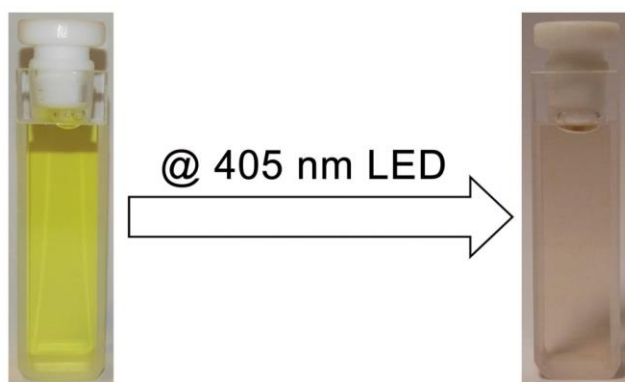


Figure S4. *In-situ* photographs for ketone-1/Iod ($3.96 \times 10^{-5} \text{ M}$ / $1.0 \times 10^{-2} \text{ M}$) two-component system dissolved in acetonitrile upon the irradiation of LED@405 nm for 10 min.

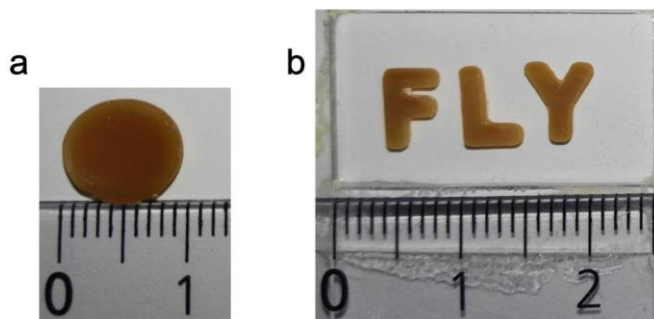


Figure S5. Photographs for TA resin containing 20% (w%) silica filler in the presence of ketone-1/amine/Iod three-component system: (a) depth of cure experiment under LED@405 nm irradiation for 5 min and (b) laser write experiment using 405 nm laser diode, respectively.